

Journal of Biomedical Optics

SPIEDigitalLibrary.org/jbo

Tryptophan autofluorescence imaging of neoplasms of the human colon

Bhaskar Banerjee
Timothy Renkoski
Logan R. Graves
Nathaniel S. Rial
Vassiliki Liana Tsikitis
Valentine Nfonsam
Judith Pugh
Piyush Tiwari
Hemanth Gavini
Urs Utzinger

Tryptophan autofluorescence imaging of neoplasms of the human colon

Bhaskar Banerjee,^{a,b,c} Timothy Renkoski,^c Logan R. Graves,^c Nathaniel S. Rial,^a Vassiliki Liana Tsikitis,^d Valentine Nfonsam,^d Judith Pugh,^e Piyush Tiwari,^a Hemanth Gavini,^a and Urs Utzinger^{b,c}

^aUniversity of Arizona, Department of Medicine, Section of Gastroenterology, 1501 N. Campbell Avenue, PO Box 245028, Tucson, Arizona 85724-5028

^bUniversity of Arizona, Department of Biomedical Engineering, 1501 N. Campbell Avenue, PO Box 245028, Tucson, Arizona 85724-5028

^cUniversity of Arizona, College of Optical Sciences, 1501 N. Campbell Avenue, PO Box 245028, Tucson, Arizona 85724-5028

^dUniversity of Arizona, Department of Surgery, 1501 N. Campbell Avenue, PO Box 245028, Tucson, Arizona 85724-5028

^eUniversity of Arizona, Department of Pathology, 1501 N. Campbell Avenue, PO Box 245028, Tucson, Arizona 85724-5028

Abstract. Detection of flat neoplasia is a major challenge in colorectal cancer screening, as missed lesions can lead to the development of an unexpected 'incident' cancer prior to the subsequent endoscopy. The use of a tryptophan-related autofluorescence has been reported to be increased in murine intestinal dysplasia. The emission spectra of cells isolated from human adenocarcinoma and normal mucosa of the colon were studied and showed markedly greater emission intensity from cancerous cells compared to cells obtained from the surrounding normal mucosa. A proto-type multispectral imaging system optimized for ultraviolet macroscopic imaging of tissue was used to obtain autofluorescence images of surgical specimens of colonic neoplasms and normal mucosa after resection. Fluorescence images did not display the expected greater emission from the tumor as compared to the normal mucosa, most probably due to increased optical absorption and scattering in the tumors. Increased fluorescence intensity in neoplasms was observed however, once fluorescence images were corrected using reflectance images. Tryptophan fluorescence alone may be useful in differentiating normal and cancerous cells, while in tissues its autofluorescence image divided by green reflectance may be useful in displaying neoplasms. © 2012 Society of Photo-Optical Instrumentation Engineers (SPIE). [DOI: 10.1117/1.JBO.17.1.016003]

Keywords: autofluorescence; colon; cancer; tryptophan.

Paper 11349 received Jul. 13, 2011; revised manuscript received Oct. 6, 2011; accepted for publication Nov. 4, 2011; published online Feb. 1, 2012; corrected Apr. 17, 2012.

1 Introduction

Colonoscopy is the preferred method of screening for colorectal cancer, however it has significant limitations.¹ Following a 'clearing' colonoscopy where all visible polyps are removed, cancerous masses are unexpectedly encountered in about 2.5 cases in 100,000 patient years within three years of colonoscopy, with devastating consequences for the patient and his caregivers.^{2,3} Although some of these cancers are due to a biological variation in growth rates, many are thought to be the result of lesions that were undetected during the colonoscopy.^{4,5} Colonoscopy is known to prevent cancers in the distal colon, but some studies have questioned its value in the proximal colon, where flat, advanced lesions can arise that are easily missed.^{4,5} Flat or superficial neoplasms were once believed to occur most commonly in Japanese patients, but the use of indigo carmine chromoendoscopy during colonoscopy revealed that such lesions are equally prevalent in the US.⁶ To be classified as flat or superficial, a lesion needs to have a height less than half its diameter; such lesions are further grouped as being slightly elevated, completely flat or depressed: the latter are most likely to harbor malignancy.⁶⁻⁸ Flat neoplasms are more commonly found in the proximal colon and have unique methylation phenotypes and *K-ras* mutations.^{6,8,9} In a recent US study,

flat neoplasms were found in 9.4% of patients undergoing colonoscopy; these neoplasms more likely to be cancerous compared to benign polypoid lesions.⁶ The contrast agent used was indigo carmine, which is a non-absorbed dye that can be sprayed on to the colonic surface using a catheter; the dye settles on grooves and pits of the mucosa to enhance topographic features not easily seen by the unaided eye.⁷ Methylene blue has also been used in chromoendoscopy, but is absorbed by mucosal cells and may cause DNA damage.¹⁰ Despite its usefulness, chromoendoscopy is a subjective and cumbersome process that is unlikely to be used during screening colonoscopy in North America and Europe, where such procedures are performed in high volume with time constraints. Recently, endoscopic narrow band imaging has been introduced, which uses blue and green illumination to display neoplastic polyps, topographical features and mucosal vasculature with high contrast, but the technique has not been shown to significantly increase the detection of polyps when compared to high resolution white light imaging.^{11,12}

Prior work on autofluorescence often used excitation greater than 330 nm resulting in a fluorescence intensity that decreases with neoplasia.^{13,14} An endoscopic autofluorescence system has been developed where blue light produces autofluorescence (490 to 625 nm) and green light (550 nm) is used to take a reflectance image of the mucosa; the autofluorescence and reflected images are pseudo-colored and overlaid on a composite image, so that

Address all correspondence to: Bhaskar Banerjee, Section of Gastroenterology, Department of Medicine, University of Arizona, 1501 N. Campbell Avenue, PO Box 245028, Tucson, Arizona 85724-5028. Tel: 520.626.3992; Fax: 520.874.7105; E-mail: bbanerjee@deptofmed.arizona.edu

reduced fluorescence from tumors appear magenta, the mucosa light green, and blood vessels dark green.¹⁵⁻¹⁷ In a tandem cross-over study, the autofluorescence imaging (AFI) system was compared to white light endoscopy in detecting polyps of the rectum and sigmoid colon in 64 patients.¹⁷ Autofluorescence imaging detected 26 (sensitivity 84%, specificity 60%) whereas white light imaging detected 28 (sensitivity 90%, specificity 64%) neoplastic lesions without any significant difference.

The broad band of visible fluorescence used in prior autofluorescence studies is believed to be from extracellular sources, including basement membrane collagen and elastin as well as cellular reduced nicotinic adenine dinucleotide (NADH) and flavin adenine dinucleotide (FAD).¹⁸⁻²⁰ The efficacy of using this wavelength range can be impacted by local inflammation and tumor invasion that can displace and disrupt the basement membrane, resulting in false-positive and false-negative results.²⁰⁻²³ At shorter excitation wavelengths, tryptophan is the predominant source of native fluorescence from cells.²⁴ Prior work has shown that its fluorescence is increased in dysplastic intestinal polyps of APC^{min+} mice and was accompanied by a higher concentration of this essential amino acid in polyp tissue compared to the surrounding normal mucosa.²⁵ Yang et al. found that emission properties of colonic adenocarcinoma can be separated from the normal colon when analyzing fluorescence spectra measured at 290 to 340 nm excitation and that the differences may be limited to tryptophan and collagen.²⁶ Acknowledging the promise of tryptophan fluorescence as a potential diagnostic target for neoplastic tissue, we examined this shorter wavelength fluorescence band in normal and cancerous cells extracted from the human colon. We also looked at its potential use as an intrinsic imaging marker for colon cancer and dysplastic polyps. Fresh surgical samples from four patients were studied and representative images are presented herein.

2 Materials and Methods

2.1 Spectroscopy of Normal and Cancerous Cells of the Colon

Full thickness 2 × 2 cm samples of the human colon were excised during surgery for colon cancer; the samples were immediately snap-frozen in liquid nitrogen and then stored at -70° Celsius. Tissue was later thawed over ice, representative samples (0.5 gram) of the tumor mass and scrapings of normal mucosa taken and cells separated from the extracellular matrix, using the method of Roediger and Truelove.²⁷ Samples of tumor and normal mucosa were also submitted for histology. Cells were then suspended in phosphate-buffered saline (PBS) at pH 7.4, which has negligible fluorescence, and placed in a quartz cuvette for measurement of emission spectra using a spectrofluorometer (Shimadzu RF-5301PC, Columbia, MD). Examination of samples of cells with trypan blue in a hemacytometer (Fisher Scientific, Pittsburgh, PA) showed similar numbers of cells in both samples (approximately 0.12 × 10⁶ cell/ml with 83% viable cells). A 150-Watt Xenon lamp provided the excitation beam, with an accuracy of ±1.5 nm, a slit width of 1.5 nm and a wavelength range of 220 to 900 nm. Excitation intensity varied with wavelength but was always less than 5 μW/mm². Cell suspensions were studied with excitation at 280 nm and emission measured from 290 to 900 nm at 1 nm increments. The emission intensity (measured in arbitrary units) was plotted on the y axis and the emission wavelength (in nanometers) on the x axis. Representative spectra

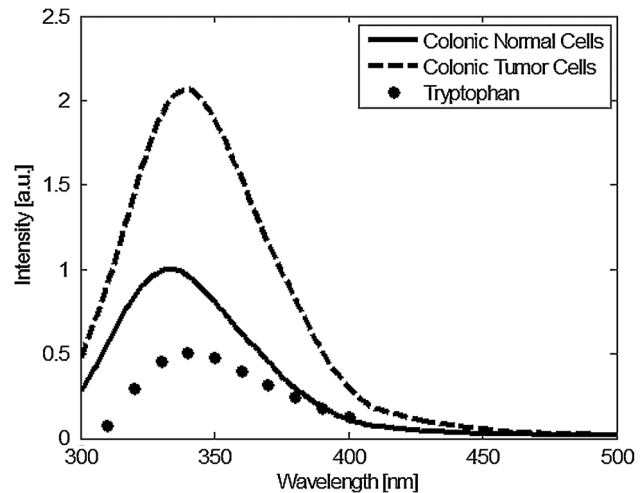


Fig. 1 Emission spectra of cells isolated from adenocarcinoma and normal mucosa and suspended in phosphate buffered saline at pH 7.4 in a quartz cuvette, along with the average emission spectrum of tryptophan. Excitation was at 280 nm and emission intensity measured from 290 nm at 1 nm increments. The y axis shows the emission intensity in arbitrary units; the x axis shows the wavelength. The average emission spectrum of tryptophan is included for comparison.

of adenocarcinoma and normal cells of the colon are shown in Fig. 1. The emission spectrum of an aqueous solution of tryptophan (Sigma-Aldrich, St. Louis, MO) was similarly recorded and is included in Fig. 1 for comparison.

2.2 Spectral Imager

A proto-type wide-field spectral imager capable of illumination from 260 to 650 nm and detection from 340 to 650 nm was constructed to measure tissue autofluorescence and reflectance over a 40-mm square field-of-view (Fig. 2). The light source was a Xenon arc lamp system (300-Watt Lambda LS, Sutter Instruments, Novato, CA) with built-in 10-position filter wheel providing bandpass-filtered excitation. The thermoelectrically cooled, UV-enhanced camera (PhotonMAX: 512B, Princeton Instruments, Trenton, NJ) used a UV-transmitting and color-corrected imaging lens ($f/3.5$, $f = 63$ mm, Resolve Optics, Chesham, UK) and had a fixed working distance of 25 cm. A custom quartz fiber bundle (FiberTech Optica, ON, Canada) delivered filtered illumination from the lamp to the specimen. A second 10-position filter wheel was mounted directly in front of the camera lens. Longpass filters were mounted in the detection filter wheel to suppress reflected excitation light reaching the camera. Fluorescence images covering a reduced emission band can be formed by subtraction of two exposures with different longpass-filtered images. With this approach the system produces at least one image with high SNR with the longpass filter at the shortest cut-on wavelength. The 280-nm excited fluorescence image, believed to be predominantly associated with tryptophan, was formed by subtracting a 410-nm longpass image from a 300-nm longpass image. Reflectance images were collected with a pair of crossed UV polarizers (Meadowlark Optics, Frederick, CO) that minimize specular reflection.

2.3 Spectral Imaging of Human Colon

Fresh surgical specimens of the colon were studied from patients undergoing elective colectomy for neoplasms of the colon.

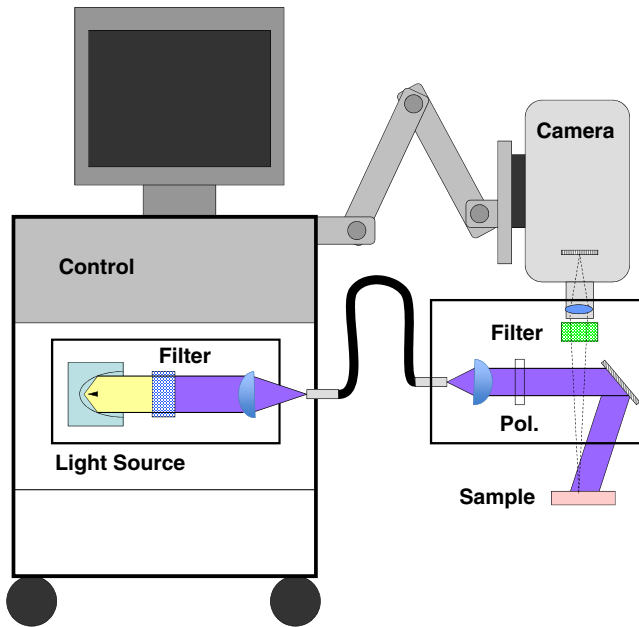


Fig. 2 System schematic: The spectral imager consists of a mobile cart containing a computer, filter wheel controller and a light source providing illumination from 260 to 650 nm through optical bandpass filters. A flexible fiberoptic cable guides the light towards the sample. To adjust the illuminated field the fiber output is collimated and reflected by a mirror towards the sample. Light emitted from the sample is collected through optical filters and imaged with an UV-objective onto a CCD camera.

A flat, raised, bi-lobed ascending colon mass in a 62-year-old Caucasian male was imaged within 40 minutes of resection (Fig. 3). A flat, raised cecal mass in a 63-year-old Caucasian female was imaged within 35 minutes of resection (Fig. 4). A pedunculated polyp in a 28-year-old Caucasian male with attenuated familial adenomatous polyposis (AFAP) and more than 25

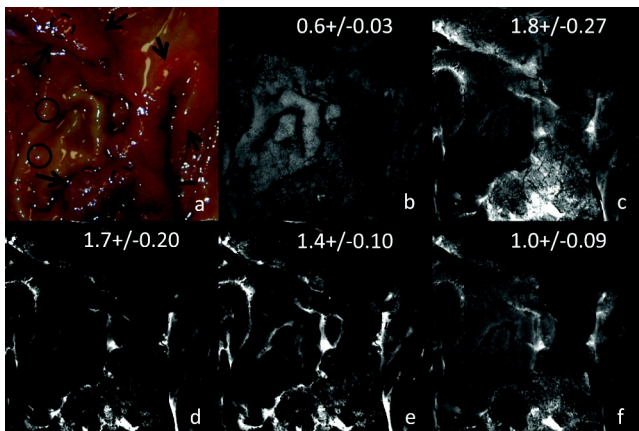


Fig. 3 (a) Color photograph of a surgical specimen of the ascending colon, showing a bi-lobed flat adenocarcinoma of the ascending colon, indicated by arrows. A 4×4 cm image of the lesion is shown with: (b) uncorrected fluorescence image at 280 nm excitation and 340 to 410 nm emission; (c) 280 nm excitation image divided by 555 nm reflectance; (d), (e), and (f) 280 nm excitation image divided by 370, 440, and 480 nm reflectance images respectively. In the encircled areas as indicated in (a), the intensity was analyzed. The average intensity ratio of the dashed (tumor) to solid (normal) areas is indicated at the top of images (b) to (f), showing highest contrast between adenocarcinoma and normal areas in (c).

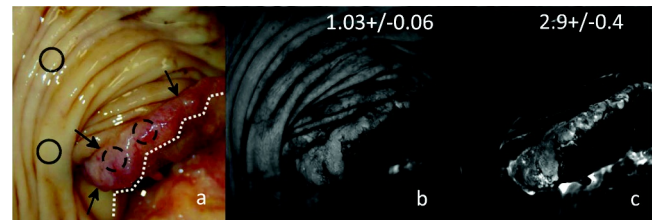


Fig. 4 (a) Color photograph of a surgical specimen showing a flat, raised adenocarcinoma of the cecum surrounded by normal mucosa (indicated with arrows). The area below the dotted white line represents mucosa that was excised and ileal mucosa and should be ignored. A 4×4 cm image of the lesion is shown with: (b) uncorrected fluorescence image at 280 nm excitation and 340 to 410 nm emission; (c) fluorescence image at 280 nm excitation divided by reflectance image at 555 nm that displayed the lesion with high contrast. In the encircled areas the intensity was analyzed. The average intensity ratio between the dashed (tumor) and solid (normal) areas is displayed at the top of (b) and (c), indicating the greatest increase in the contrast between cancerous and normal mucosa in (c).

polyps was imaged within 40 minutes of resection of the colon (Fig. 5).²⁸ The depth of sub-surface fluorescence was studied in a flat, raised lesion in the rectum of a 77-year-old Caucasian man by making an incision through the tumor, illuminating the mucosal surface with a fiberoptic probe and imaging the cut surface at 90 degrees to the illumination (Fig. 6). Specimens were collected following resection, transported to the imaging laboratory and irrigated with normal saline to remove stool and/or blood. A color image was taken of each specimen with a digital camera (Nikon D100, Nikon Inc., Melville, NY). Each specimen was then illuminated at 280 nm and the autofluorescence images recorded with the proto-type spectral imager. Reflectance images were captured at 340, 370, 400, 415, 440, 480, and 555 nm. Intrinsic autofluorescence images were approximated by dividing autofluorescence images by reflectance images. In the resulting images, the fluorescence intensity was analyzed within two approximately 5-mm diameter circular areas of the tumor and normal mucosa and the tumor-to-normal mucosa intensity ratio calculated. Informed consent was obtained from all patients prior to surgery, and the study was approved by the Institutional Review Board.

3 Results

Cellular emission spectra collected with the spectrofluorometer showed a peak at 330 to 340 nm when excited at 280 nm consistent with the emission of tryptophan (Fig. 1). The fluorescence



Fig. 5 (a) Color photograph of a 15-mm diameter pedunculated adenomatous polyp in the ascending colon of a surgical specimen from a patient with AFAP. A 4×4 cm image of the lesion is shown with: (b) uncorrected fluorescence image at 340 to 410 nm; (c) final image after fluorescence image was divided by reflectance image at 555 nm, with greater intensity of fluorescence in the head of the polyp. The average intensity ratio between the dashed (polyp) and solid (normal) areas is displayed at the top of (b) and (c), indicating an increase in the contrast between cancerous and normal mucosa in (c).

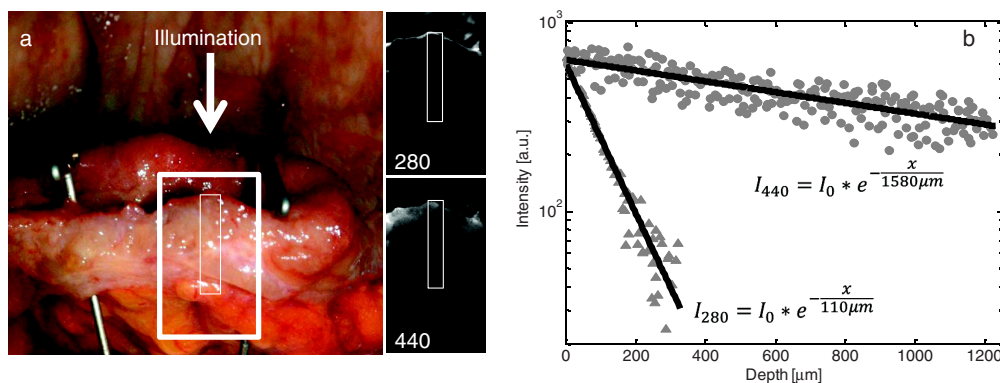


Fig. 6 Depth of fluorescence. (a) The color photograph illustrates a surgical specimen of a flat, raised, adenocarcinoma of the rectum, where the tumor was cut vertically and positioned with pins to expose the cut surface to the camera. The specimen was illuminated horizontally as indicated by the white arrow and the cut surface imaged from above, perpendicular to the illumination. Grayscale images of the large rectangular area in the color image are shown to the right, with a steep fluorescence decay at 280-nm excitation and a gradual decay at 440-nm excitation. (b) Intensity profiles were extracted within the small rectangular areas and the data plotted to the right. The intensity decay followed an exponential curve with the $1/e$ decay at 110 microns for 280 nm excitation and 1.6 mm at 440 nm excitation.

spectrum of tryptophan is included in Fig. 1 for comparison and represents the average of an aqueous solution of tryptophan as well as spectra from Chen et al and Lindsey et al.^{29,30} The peak emission from cancerous cells was about twice that of normal cells from the same colon (Fig. 1). Microscopy of adjacent tissue samples confirmed the presence of a moderately differentiated adenocarcinoma and normal mucosa.

Figure 3(a) shows a color image of a surgical specimen with a flat, elevated, bi-lobed neoplasm of the ascending colon, about 5 cm long in its greatest dimension, with its borders indicated by arrows. The uncorrected autofluorescence image (excitation 280 nm, emission from 340 to 410 nm) exhibited unremarkable contrast with intensity lower than that of the surrounding mucosa [Fig. 3(b)]. We investigated dividing the autofluorescence image by reflectance images at each of seven wavelengths from 340 to 555 nm. Autofluorescence images divided by the corresponding reflectance images at 555 nm, 370 nm, 440 nm and 480 nm are shown in Figs. 3(c), 3(d), 3(e) and 3(f) respectively. The image produced by using reflectance at 555 nm [Fig. 3(c)] exhibited the contrast most useful of all seven wavelengths for identifying this flat lesion. The tumor- to -normal mucosa image intensity ratio was greatest (1.8 ± 0.27) when the fluorescence image was divided by 555 nm and the ratio was least in the uncorrected image (0.6 ± 0.03). Tissue microscopy of the lesion of Fig. 3 confirmed a moderately differentiated adenocarcinoma.

The color image of a second surgical sample containing a flat, raised 3-cm long mass in the cecum, close to the ileocecal valve with the borders indicated by arrows, is shown in Fig. 4(a). A portion of this tumor had been excised for another research project immediately prior to imaging and the cut margin is indicated by dotted lines. The corresponding uncorrected grayscale autofluorescence image in Fig. 4(b) shows intensity at the tumor that is comparable to the surrounding mucosa; the average fluorescence intensity ratio between tumor and normal areas was 1.03 ± 0.06 [Fig. 4(b)]. The autofluorescence image divided by the 555-nm reflectance image showed the greatest overall contrast and the highest average image intensity ratio of 2.9 ± 0.4 [Fig. 4(c)]. Fluorescence images divided by other reflectance wavelengths are not shown. Tissue microscopy of the lesion depicted in Fig. 4 confirmed a moderately to well-differentiated adenocarcinoma of the colon.

Images from a third specimen, showing a 15-mm diameter pedunculated polyp in the ascending colon of a patient with an attenuated familial adenomatous polyposis (AFAP) are presented in Fig. 5. The pedunculated polyp shows unremarkable contrast in the uncorrected tryptophan-associated fluorescence image [Fig. 5(b)], with an average image intensity ratio of 0.97 ± 0.12 ; however, the image is greatly enhanced when divided by the reflectance image at 555 nm, with an average image intensity ratio of 3.0 ± 0.6 [Fig. 5(c)]. Contrast enhancement is greatest in the head of the dysplastic polyp and not the stalk, which contains normal tissue. The histology of the polyp showed a tubular adenoma, which is dysplastic.

Imaging of the final specimen (Fig. 6) shows a color image of a 4-cm diameter, flat, raised neoplasm of the rectum, cut vertically through the mass and positioned to expose the cut surface to the camera located vertically above. The specimen was illuminated with a fiberoptic probe positioned horizontally and did not illuminate the surface being imaged. The fluorescence images obtained from the cut surface showed fluorescence

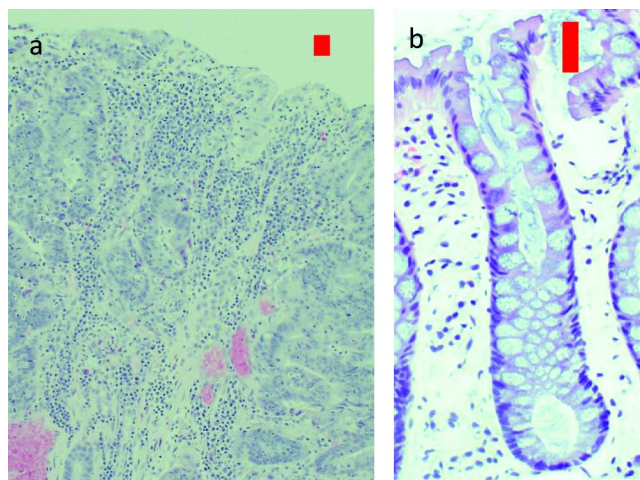


Fig. 7 Cross-sectional histology using hematoxylin and eosin stain showing: (a) the invasive adenocarcinoma (magnification $\times 40$) imaged in Fig. 6; and (b) an example of the normal mucosa of the colon displaying a single crypt (magnification $\times 100$). Red bars in each image indicate a depth of about 110 microns.

limited to the epithelial surface of the lesion when illuminated at 280 nm, but extended to a greater depth at 440 nm. The intensity decay followed an exponential curve with the $1/e$ decay at 110 microns for 280 nm and 1.6 mm for 440 nm excitation. The histology of this specimen (magnification $\times 40$) showed a moderately differentiated adenocarcinoma [Fig. 7(a)] and for comparison, the cross sectional histology of the normal colon with a crypt is (magnification $\times 100$) shown in Fig. 7(b). Red bars indicate a distance of about 110 microns. A similar result was found on a second colon cancer specimen with decay to $1/e$ at 100 microns for 280 nm and 2.5 mm for 440 nm excitation (image not presented).

4 Discussion and Conclusions

Our preliminary study indicates the diagnostic potential of using tryptophan fluorescence to differentiate cancerous cells of the colon from normal colonocytes. In surgical specimens of colon cancer, the macroscopic tryptophan-associated fluorescence image displays the greatest contrast compared to the surrounding normal mucosa when divided by a reflectance image. This method of correction by reflectance enabled tumors to be imaged with two to three times the intensity of the surrounding normal mucosa. Our hypothesis is that this imaging modality provides a novel contrast mechanism that may be useful in preventing flat neoplasm from being missed.

The tryptophan-related fluorescence from cancerous cells was about twice that in normal cells, both isolated from the same human colon. The fluorescence spectra of cells is comparable to that of tryptophan (Fig. 1). The only other tissue molecule known to fluoresce at this wavelength range is collagen, which is part of the extracellular matrix and therefore not present in cells.^{19,20}

In comparison, the uncorrected fluorescence was attenuated in the adenocarcinomas and a dysplastic polyp, with image intensities comparable to or less than the surrounding normal mucosa. This attenuated fluorescence in neoplastic tissue, compared to the large difference observed between cancerous and normal cells may be due to changes in tissue mass, structure, scattering and absorption. Neoplastic transformation in the colon is accompanied by an increase in mass, cell density, as well as angiogenesis, which allows tumors to grow and metastasize.³¹⁻³⁴ The hypervascular nature of the tumors and the polyp studied is represented by the color images of the specimens, Figs. 3-5(a), with hypervascular areas appearing as bright red. To compensate for tissue optical absorption and scattering, we approximated intrinsic fluorescence with fluorescence divided by cross-polarized reflectance collected at a wavelength longer than the fluorescence emission. This is similar to methods described by Zeng et al.³⁵ and Qu et al.³⁶ Comparison of the autofluorescence images corrected by each of the seven different wavelength reflectance images showed the best results when the fluorescence images were divided by reflectance at the longest wavelengths studied, which are absorbed less readily by hemoglobin.³⁷ This might be expected, as correction of fluorescence spectra by diffuse reflectance spectra has been shown to be inaccurate for high -absorption conditions, such as those caused by pooled blood.^{38,39} Our results indicate that dividing by an ultraviolet or blue reflectance image results in overcorrection of autofluorescence in areas where tissue is not normal to observation and from hypervascular regions [Figs. 3(d) and 3(e)]. While the intensity ratio between tumor and normal areas were increased at all reflectance wavelengths compared to the uncorrected

image, division by 555 nm reflectance produced the largest contrast and also highlighted subtle changes in vascularity as well as a greater heterogeneity in the neoplastic areas compared to the normal background [Figs. 3-5(c)]. As a neoplasm progresses from dysplasia to cancer, it increases in bulk and becomes more vascular, which leads to greater absorption of the cellular fluorescence, resulting in a decrease in net fluorescence that can be partly corrected by the technique described.^{40,41} Establishing the validity of this method as a means of recovering intrinsic fluorescence would require a phantom study but that is not the primary goal of this work. The usefulness of this correction for improving lesion contrast is evidenced by the images presented here. Further, the degree of absorption by hemoglobin may have been affected by the brief interval of loss of blood flow and oxygenation from the time of surgery, and further adjustment may be needed to optimally image such lesions *in-vivo*.

Although the Olympus Autofluorescence Imaging (AFI) system shows striking color contrast between tumors and normal mucosa, its performance in detecting neoplastic polyps was not superior to white light endoscopy in a small study population; it seemed to miss fewer flat lesions, but not significantly.¹⁷ Further, polyp size and classification are not provided and the study was limited to the rectum and distal sigmoid colon, whereas flat neoplasms are encountered most commonly in the proximal colon.^{8,42-44} Our imaging technique is distinctively different from both AFI and Light Induced Fluorescence Endoscopy (LIFE) systems as we excite and observe in the ultra violet (UV) range.¹⁵⁻¹⁷ Further, AFI displays reflectance and fluorescence concurrently in two separate color channels, and LIFE uses a green/red fluorescence ratio in contrast to our method where the fluorescence image is divided by the green reflectance image.¹⁵⁻¹⁷ The autofluorescence image in the LIFE and AFI depends on cellular and extracellular fluorophores, including NADH, FAD, collagen and elastin as well as the effects of absorption and scattering. The presence of inflammation with tissue edema or minimal interruption of the basement membrane by a malignant process can both reduce its sensitivity and specificity for detecting gastrointestinal neoplasms.^{22,45} Nevertheless our work represents a preliminary, qualitative *in-vitro* study on surgical specimens, indicating the potential advantages of this UV technique in detecting flat neoplasms; it cannot be compared directly to an *in-vivo* endoscopic study.

When imaging in the UV, transmission of light through standard optical materials is usually limited to 380 nm and to 340 nm with optimized components. Imaging below these wavelengths requires specialized UV optics. Optical band pass filters with transmission bands below 350 nm provide a further challenge because of their reduced ability to block out-of-band light that might interfere with the observed fluorescence. Illumination channels also require UV optimized fiber optics.

Although the effect of UV light on intestinal mucosa is not known, imaging in the mid-UV may impose a risk for UV photo toxicity.⁴⁶ However, our previous work illustrates that it is possible to record fluorescence spectra of living tissues with excitation below 300 nm while staying below the safety threshold limits.⁴⁷ The total exposure in those studies was in the range of 20% of the threshold limit value and we expect an optimally constructed imaging device to fall within the same range of UV exposure.⁴⁶ The safety of using UV illumination will have to be investigated by carefully designed *in vivo* studies. However, we anticipate that due to UV exposure restrictions, prolonged

mid-UV video endoscopy may not be feasible and necessitate the use of a single exposure still image that can be compared to or superimposed on the white light video endoscopic image. Therefore we do not believe that photo bleaching is relevant for this imaging configuration.

As depicted in Fig. 6, illumination with 280 nm results in tissue fluorescence and hence penetration to a depth of about 100 microns below the surface, compared to the much greater depth of 1.6 to 2.5 mm when illuminating at 440 nm. The cells lining the mucosa of the colon have their origins in the crypts. Stem cells at the base of the crypts divide to give rise to colonocytes that migrate up to the epithelium before being shed into the lumen to form stool, a process that takes about a week to complete.^{48–50} The cells at greatest risk from photo-toxicity are the stem cells at the base of the crypts, which are about 50 cells deep.⁵¹ The base of the crypts lie about 500 microns below the luminal surface and are beyond the approximately 100 microns of tissue penetrated by 280-nm illumination.⁵² The red bars in Fig. 7 indicate the approximate depth of penetration of 280-nm illumination. With 280-nm illumination, only superficial epithelial cells of the crypts of the normal colon would be excited, probably no more than about two days before they are discarded into the colonic lumen as stool. In contrast, illumination with 440 nm would excite the entire length of the crypts. With UV illumination, one would expect limited contribution to the fluorescence from collagen in the basement membrane of the normal mucosa, but in cancer, this sheet-like fibrous platform may be disrupted or displaced beyond the reach of UV illumination and will contribute little, if any, to the fluorescence image.

Our preliminary results indicate that tryptophan fluorescence may be used to differentiate cancerous cells from normal cells of the colon and that our imaging modality provides a novel contrast mechanism that should be investigated further to help address the problem of missed flat neoplasms of the colon and other organs.

References

- D. K. Rex, "Colonoscopy: the dominant and preferred colorectal cancer screening strategy in the United States," *Mayo Clin. Proc.* **82**(6), 662–664 (2007).
- N. N. Baxter et al., "Association of colonoscopy and death from colorectal cancer," *Ann. Intern. Med.* **150**(1), 1–8 (2009).
- D. J. Robertson et al., "Colorectal cancer in patients under close colonoscopic surveillance," *Gastroenterology* **129**(1), 34–41 (2005).
- D. K. Rex, "Maximizing detection of adenomas and cancers during colonoscopy," *Am. J. Gastroenterol.* **101**(12), 2866–2877 (2006).
- D. K. Rex, D. G. Hewett, and D. C. Snover, "Editorial: Detection targets for colonoscopy: from variable detection to validation," *Am. J. Gastroenterol.* **105**(12), 2665–2669 (2010).
- R. M. Soetikno et al., "Prevalence of nonpolypoid (flat and depressed) colorectal neoplasms in asymptomatic and symptomatic adults," *JAMA* **299**(9), 1027–1035 (2008).
- S. Kudo et al., "Colonoscopic diagnosis and management of nonpolypoid early colorectal cancer," *World J. Surg.* **24**(9), 1081–1090 (2000).
- R. Lambert, "Update on the Paris classification of superficial neoplastic lesions in the digestive tract," *Endoscopy* **37**(6), 570–578 (2005).
- S. Hiraoka et al., "Laterally spreading type of colorectal adenoma exhibits a unique methylation phenotype and *K-ras* mutations," *Gastroenterology* **131**(2), 379–389 (2006).
- J. Davies et al., "Methylene blue but not indigo carmine causes DNA damage to colonocytes in vitro and in vivo at concentrations used in clinical chromoendoscopy," *Gut* **56**(1), 155–156 (2007).
- D. K. Rex and C. C. Helbig, "High yields of small and flat adenomas with high-definition colonoscopes using either white light or narrow band imaging," *Gastroenterology* **133**(1), 42–47 (2007).
- A. Adler et al., "Narrow-band versus white-light high definition television endoscopic imaging for screening colonoscopy: a prospective randomized trial," *Gastroenterology* **136**(2), 410–416 (2009).
- K. T. Schomacker et al., "Ultraviolet laser-induced fluorescence of colonic tissue: basic biology and diagnostic potential," *Lasers Surg. Med.* **12**(1), 63–78 (1992).
- B. Mayinger et al., "Endoscopic light-induced autofluorescence spectroscopy for the diagnosis of colorectal cancer and adenoma," *J. Photochem. Photobiol. B* **70**(1), 13–20 (2003).
- N. Nakaniwa et al., "Newly developed autofluorescence imaging videoendoscopy system for the detection of colonic neoplasms," *Digest Endosc.* **17**, 235–240 (2005).
- N. I. Uedo et al., "Novel autofluorescence videoendoscopy imaging system for diagnosis of cancers in the digestive tract," *Digest Endosc.* **18**(Suppl. 1), S131–S136 (2006).
- N. Uedo et al., "Diagnosis of colonic adenomas by new autofluorescence imaging system: A pilot study," *Digest Endosc.* **19**, S134–S138 (2007).
- K. T. Schomacker et al., "Ultraviolet laser-induced fluorescence of colonic polyps," *Gastroenterology* **102**(4), 1155–1160 (1992).
- B. Banerjee, B. Miedema, and H. R. Chandrasekhar, "Emission spectra of colonic tissue and endogenous fluorophores," *Am. J. Med. Sci.* **316**(3), 220–226 (1998).
- B. Banerjee, B. E. Miedema, and H. R. Chandrasekhar, "Role of basement membrane collagen and elastin in the autofluorescence spectra of the colon," *J. Invest. Med.* **47**(6), 326–332 (1999).
- T. D. Wang et al., "In vivo identification of colonic dysplasia using fluorescence endoscopic imaging," *Gastrointest. Endosc.* **49**(4), 447–455 (1999).
- M. A. Kara et al., "A randomized crossover study comparing light-induced fluorescence endoscopy with standard videoendoscopy for the detection of early neoplasia in Barrett's esophagus," *Gastrointest. Endosc.* **61**(6), 671–678 (2005).
- A. R. Mackay et al., "Basement membrane type IV collagen degradation: evidence for the involvement of a proteolytic cascade independent of metalloproteinases," *Cancer Res.* **50**(18), 5997–6001 (1990).
- N. D. Kirkpatrick et al., "Endogenous fluorescence spectroscopy of cell suspensions for chemopreventive drug monitoring," *Photochem. Photobiol.* **81**(1), 125–134 (2005).
- B. Banerjee et al., "Detection of murine intestinal adenomas using targeted molecular autofluorescence," *Dig. Dis. Sci.* **49**(1), 54–59 (2004).
- Y. Yang et al., "Fluorescence spectroscopy as a photonic pathology method for detecting colon cancer," *Lasers Life Sci.* **6**(4), 259–276 (1995).
- W. E. Roediger and S. C. Truelove, "Method of preparing isolated colonic epithelial cells (colonocytes) for metabolic studies," *Gut* **20**(6), 484–488 (1979).
- G. S. Hemegger, H. G. Moore, and J. G. Guillem, "Attenuated familial adenomatous polyposis: an evolving and poorly understood entity," *Dis. Colon Rectum* **45**(1), 127–134; discussion 134–126 (2002).
- R. F. Chen, "Fluorescent protein-dye conjugates. II. Gamma globulin conjugated with various dyes," *Arch. Biochem. Biophys.* **133**(2), 263–276 (1969).
- J. S. Lindsey et al., "PhotochemCAD: A computer-aided design and research tool in photochemistry," *Photochem. Photobiol.* **68**(2), 141–142 (1998).
- Y. Kondo et al., "Enhancement of angiogenesis, tumor growth, and metastasis by transfection of vascular endothelial growth factor into LoVo human colon cancer cell line," *Clin. Cancer Res.* **6**(2), 622–630 (2000).
- R. M. Shaheen et al., "Inhibited growth of colon cancer carcinomatosis by antibodies to vascular endothelial and epidermal growth factor receptors," *Br. J. Cancer* **85**(4), 584–589 (2001).
- B. St Croix et al., "Genes expressed in human tumor endothelium," *Science* **289**(5482), 1197–1202 (2000).
- D. J. Faber et al., "Light absorption of (oxy-)hemoglobin assessed by spectroscopic optical coherence tomography," *Opt. Lett.* **28**(16), 1436–1438 (2003).

35. H. Zeng et al., "Spectroscopic and microscopic characteristics of human skin autofluorescence emission," *Photochem. Photobiol.* **61**(6), 639–645 (1995).
36. J. Y. Qu and J. W. Hua, "Calibrated fluorescence imaging of tissue in vivo," *Appl. Phys. Lett.* **78**(25), 4040–4042 (2001).
37. B. Horecker, "The absorption spectra of hemoglobin and its derivatives in the visible and near infra-red regions," *J. Biol. Chem.* **148**, 173–183 (1943).
38. R. S. Bradley and M. S. Thorniley, "A review of attenuation correction techniques for tissue fluorescence," *J. R. Soc. Interface* **3**(6), 1–13 (2006).
39. W. G. Zijlstra, A. Buursma, and W. P. Meeuwssen-van der Roest, "Absorption spectra of human fetal and adult oxyhemoglobin, de-oxyhemoglobin, carboxyhemoglobin, and methemoglobin," *Clin. Chem.* **37**(9), 1633–1638 (1991).
40. J. Folkman and R. Cotran, "Relation of vascular proliferation to tumor growth," *Int. Rev. Exp. Pathol.* **16**, 207–248 (1976).
41. R. E. Frank et al., "Tumor angiogenesis as a predictor of recurrence and survival in patients with node-negative colon cancer," *Ann. Surg.* **222**(6), 695–699 (1995).
42. B. Iacopetta, "Are there two sides to colorectal cancer?," *Int. J. Cancer* **101**(5), 403–408 (2002).
43. C. Cucino, A. M. Buchner, and A. Sonnenberg, "Continued rightward shift of colorectal cancer," *Dis. Colon Rectum* **45**(8), 1035–1040 (2002).
44. H. Singh et al., "The reduction in colorectal cancer mortality after colonoscopy varies by site of the cancer," *Gastroenterology* **139**(4), 1128–1137 (2010).
45. R. G. Rowe and S. J. Weiss, "Navigating ECM barriers at the invasive front: the cancer cell-stroma interface," *Ann. Rev. Cell Devel. Biol.* **25**, 567–595 (2009).
46. R. Matthes et al., "Guidelines on limits of exposure to ultraviolet radiation of wavelengths between 180 nm and 400 nm (incoherent optical radiation)," *Health Phys.* **87**(2), 171–186 (2004).
47. R. George et al., "Clinical research device for ovarian cancer detection by optical spectroscopy in the ultraviolet C-visible," *J. Biomed. Opt.* **15**(5), 057009 (2010).
48. E. Marshman, C. Booth, and C. S. Potten, "The intestinal epithelial stem cell," *BioEssays: news and reviews in molecular, cellular and developmental biology* **24**(1), 91–98 (2002).
49. V. Lorenzo and J. S. Trier, "Fine structure of human rectal mucosa—epithelial lining of base of crypt," *Gastroenterology* **55**(1), 88–101 (1968).
50. S. Tsubouchi and C. P. Leblond, "Migration and turnover of entero-endocrine and caveolated cells in the epithelium of the descending colon, as shown by radioautography after continuous infusion of 3H-thymidine into mice," *Am. J. Anat.* **156**(4), 431–451 (1979).
51. C. R. Daniel et al., "TGF- α expression as a potential biomarker of risk within the normal-appearing colorectal mucosa of patients with and without incident sporadic adenoma," *Cancer Epidemiol. Biomarkers Prev.* **18**(1), 65–73 (2009).
52. A. McTiernan et al., "Effect of a 12-month exercise intervention on patterns of cellular proliferation in colonic crypts: a randomized controlled trial," *Cancer Epidemiol. Biomarkers Prev.* **15**(9), 1588–1597 (2006).